THE UNIVERSITY OF ALBERTA

OXIDATION OF STIBNITE

A THESIS

SUBMITTED TO THE FACULTY OF GRADUATE STUDIES
IN PARTIAL FULFILMENT OF THE REQUIREMENTS FOR THE
DEGREE OF MASTER OF SCIENCE

DEPARTMENT OF MINING AND METALLURGY

BY

RICHARD ALWYN BRAMLEY-MOORE

EDMONTON, ALBERTA

AUGUST, 1960

TABLE OF CONTENTS

ABSTRACT

A design and method of construction of a vertical tube furnace and auxiliary equipment including a quartz spring balance to measure weight changes of samples in the furnace are given.

The oxidation of stibnite is studied over the temperature range 300°C to 750°C, oxygen partial pressures 35 to 245 mm. of Hg and low gas flows (from 5 to 50 ml./min.).

The antimony oxide formed during the oxidation of stibnite is either antimony trioxide, or antimony tetraoxide or both. These are both solids and are not removed from the sphere of roasting.

The rate of the oxidation of stibnite is controlled by two or possibly three processes between 300°C and 700°C. At low temperatures (300°C to 350°C) the reaction rate was found to be controlled by adsorption of oxygen onto the solid. From 400°C to 500°C the rate determining step was found to be probably diffusion of the oxygen through a porous layer of antimony oxide on the sample. Above the melting point of stibnite (550°C) the rate determining process could be either adsorption of the oxygen or the reaction at the surface.

The activation energy for the oxidation of stibnite below and above its melting point was found of the order of 20 and 30 kcal./mole respectively.

ACKNOWLEDGEMENTS

The investigations described in this thesis were carried out in the laboratories of the Department of Mining and Metallurgy under the supervision of Professor E.O. Lilge and Dr. J. Leja.

The author also wishes to thank the other members of the Department of Mining and Metallurgy, in particular, Dr. W. V. Youdelis for assistance in the field of rate theory.

Grateful acknowledgement is made to Eldorado Mining and Refining Limited for the financial assistance given to the writer in the form of research assistantships both in the first and second years of his Master's program.

LIST OF TABLES

LIST OF FIGURES

INTRODUCTION

The purpose of this investigation was to study the oxidation of stibnite, i.e., antimony trisulfide (Sb_2S_3). This mineral was chosen because, as a common constituent of gold ores, it causes considerable difficulties in treating antimonial gold ores by cyanidation[21] [22] [23]. Despite this, published information on the oxidation of stibnite is lacking. Up to the present, some operators have been of the opinion that antimony can be removed from an ore by roasting [21] [23].

The main object of this work was to prove or disprove this assumption and if removal of antimony is possible by roasting to find the conditions where all of the products of stibnite would be removed as gases.

The procedure adopted for this investgation was to study the oxidation of multicrystalline briquets of stibnite. This was done using a furnace in which the atmosphere was controlled and also using a quartz spring balance to measure the weight changes of the samples as the oxidation took place.

PREVIOUS WORK

Very little information could be found in literature on the subject of oxidation of antimony sulfides.

Cazafura[1] attempted to explain the chemistry of roasting by means of a differential thermal analysis, combined with chemical analysis data of the products obtained from roasting sulfides at specified

temperatures.

He showed the following relationships for antimony trisulfide:

Sb_2S_3 (crystalline) + $9/2O_2$ = Sb_2O_3 + $3SO_2$; ΔH_{298} = -340.02 kcal.
ΔF_{298} = -324.14 kcal.

Sb_2O_3 + $1/2O_2$ = Sb_2O_4; ΔH_{298} = -47.6 kcal.
ΔF_{298} = -40.6 kcal.

Figure 1 shows Cazafura's plot of enthalpy vs. time for the oxidation of diantimony trisulfide. This curve shows the two steps of oxidation of Sb_2S_3 to Sb_2O_3 and to Sb_2O_4. The sulfur dioxide was eliminated in the first step.

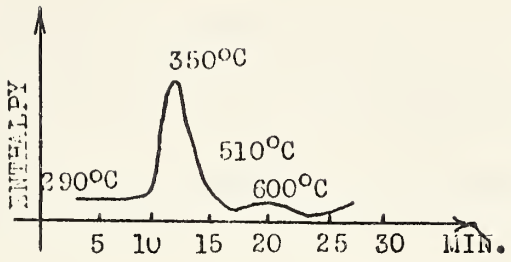

FIGURE 1 - PLOT OF ENTHALPY VS. TIME FOR THE OXIDATION OF DIANTIMONY TRISULFIDE (AFTER CAZAFURA [1])

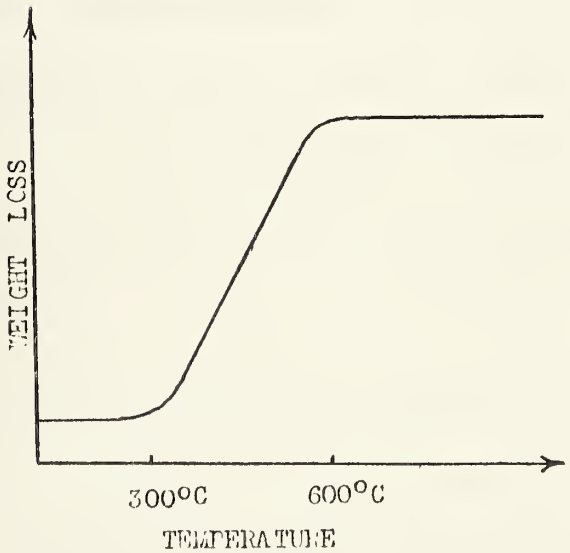

FIGURE 2 - CURVE SHOWING THE DECOMPOSITION OF STIBNITE (AFTER CHARRIER [2])

Cazafura stated that the process of oxidation of sulfides could be divided into two stages. The reactions which occured between the sulfide and the oxygen belonged to the first stage, and the reactions which took place between the products of the first stage and the underlying unchanged sulfide (on solid/solid contact surfaces) belonged to the second stage.

As electronic conductors, the sulfides must have a surplus of electrons which could only be provided by a prevalence of metal or sulfur ions. Chemisorption of oxygen may take place, resulting in the formation of oxygen ions, or a direct substitution of sulfur ions or atoms by oxygen, leading to the formation of sulfur dioxide, which leaves the solid phase and enters the gaseous phase. Which reaction prevails in the first stage is determined by different factors like the type of unit cell, the diameter of the metal atom, and the strength of the chemical bond.

Charrier [2] studied the decomposition of various sulfide minerals by using thermal analysis. He determined for each mineral studied the curves of variation of weight as a function of temperature, using a progressive rise of temperature at a rate of 7 to 8°C per minute. The mineral was crushed to 150 mesh and distributed on a flat cupel in a thin bed, two to three millimeters in thickness. Figure 2 shows the decomposition of a stibnite sample from Sierra Morena, obtained by Charrier. It indicates a nearly continuous loss of weight between 300

and 600°C.

Charrier also stated that the constituent antimony trisulfide present in tetrahedrite ($4Cu_2S \cdot Sb_2S_3$) is oxidized at a temperature between 430° and 480°C to Sb_2O_3. He assumed that the mineral undergoes a structural regrouping equivalent to a dissociation into the simple compounds Cu_2S and Sb_2S_3 at about 430°C.

No other paper appears to deal directly with the oxidation of stibnite. Papers on roasting in general or on oxidation of other minerals are, however, more numerous.

Kellogg [3] gave the main roasting reaction as:

$$MS\ (s) + 3/2O_2 = MO\ (s) + SO_2$$

He stated that for all metal sulfides this reaction is strongly exothermic and the equilibrium position is far to the right. Since the reaction is exothermic, the equilibrium shifts in the right-to-left direction as the temperature is raised. However, at all practical temperatures of roasting (between 500° and 1200°C), the amount of this shift is small and the equilibrium position remains far to the right. The main roasting reaction is essentially irreversible. Analysis of the factors that influence the rate of this reaction showed that:

1. The rate increased rapidly with increased temperature.
2. The rate was proportional to the partial pressure of oxygen at the surface of the reacting particle. Because of diffusion effects, the partial pressure of oxygen at the particle surface

may be considerably lower than in the bulk of the roaster gas. For this reason, intimate contact between gas and solid and a high relative velocity between gas and solid markedly increase the rate of reaction.

3. The rate was proportional to the surface area of metal sulfide.

Among gaseous constituents there is only one equilibrium of importance. This is the reaction:

$$SO_2 + 1/2O_2 = SO_3$$

This reaction is exothermic. The standard free energy is given by Kellogg [3] as $\Delta F^\circ = 21600 + 2.305\ T \log T + 13.44\ T$. At low temperatures (below 500°C) the equilibrium of the above reaction in an oxidizing atmosphere is shifted predominantly to the right (SO_3 is stable). However, the rate of this gaseous reaction is very slow at low temperatures, and a catalyst is required to obtain appreciable rates of formation of SO_3 from SO_2 and O_2. At higher temperatures (above 700°C) the equilibrium of this reaction is shifted to the left (SO_2 is more stable) but finite amounts of SO_3 are still present. Moreover, the rate of this reaction is appreciable above 700°C, especially in the presence of certain metallic oxides which are catalysts for the reaction, so that roaster gases contain nearly equilibrium proportions of SO_2 and SO_3. Since this reaction involves a change in the number of moles of gas, the equilibrium is pressure sensitive. Higher total pressure or lower content of inert gases at constant pressure has the effect of shifting the

equilibrium of this reaction to the right, toward a greater proportion of SO_3. The proportion of the inert diluent gases must therefore be known in order to predict the proportions of SO_2 and SO_3 in roaster gases. Diev et al[7] stated that SO is kinetically important as an intermediate oxidation product of sulfur.

Kellogg [3] also stated that in addition to simple metallic oxides such as MO, etc., and unreacted metal sulfides, roaster solids may contain MSO_4, $MO \cdot MSO_4$, MSO_3, $MO \cdot M_2O_3$, etc. In a system containing SO_2 and MO, the formation of metal sulfites is possible, however, the sulfites of the common metals are all unstable at practical roasting temperatures (>600°C), so that these compounds are not found in the roaster calcine. Roaster calcine often contains complex oxides. These compounds may be undesirable constituents in a calcine because of their low solubility in acids and the difficulty of reduction to the metallic state. At roaster temperatures, the formation of most of these compounds from the simple oxides is spontaneous, and the equilibrium cannot be reversed under practical conditions. The degree of formation of complex oxides in a calcine can only be reduced by factors which decrease the rate of solid-solid reaction -- lower temperature, less intimate mixture of the individual oxides, lower residence time in the roaster, etc.

Dannatt and Ellingham [4] stated that for reactions occurring at an interface between two phases, the rates at which reactants could be

brought to the interface and products removed from it, often determine the velocity of the reaction as a whole. In such cases the reaction velocity might be increased by movement of the fluid phase or phases, e.g., by causing a liquid or gaseous reactant to flow across the surface of a solid reactant. In such processes, however rapid is the streaming there is always a stationary fluid film in contact with the solid, through which the transport of reactants and products must be maintained by diffusion, and, in reactions between a gas and a porous solid, diffusion through the gas filled pores might also intervene between the gas stream and the inner solid surfaces at which the reaction mainly occurs. If in a gas-solid reaction there is a gaseous product as well as a gaseous reactant, the continuous removal of the former from the sphere of action in a gas stream may have an important effect on the velocity of the whole process, for the partial pressure of the gaseous product at the surface of the solid may be kept down to an extremely low value. By this means, reactions that would be thermodynamically impossible with the gaseous participants at atmospheric pressure may be made to proceed rapidly.

Peretti [5] stated that the most probable roasting reactions could be summed as follows:

$$MS_2(s) = MS(s) + 1/2S_2(g)$$

$$1/2S_2(g) + O_2(g) = SO_2(g)$$

$$MS(s) + 3/2O_2(g) = MO(s) + SO_2(g)$$

Polyvyannyi [6] showed that the rate of oxidation and desulfurization was faster for amorphous than for crystalline products.

Thornhill and Pidgeon [8] have shown that the mobility of cationic species in a sulfide is much greater than that of the anions, so that it might be expected that if diffusion in the sulfide played a part in the roasting reactions, the metal component of the sulfide could be oxidized more rapidly than the sulfur, leaving a sulfide kernel having a higher sulfur-to-metal ratio than that of the original mineral. This can, of course, occur only in sulfides which can exist over a wide range of composition.

Ong et al [9] showed that for the oxidation of sphalerite, the absolute rate of reaction depended on the concentration of reactive surface sites and became constant as the ratio of the number of reactive surface sites available approached unity. At higher temperatures, however, the disporportionately higher rates were observed and were found to have been due to self-heating of the sample; this may occur at some temperature range for all exothermic processes. Self-heating is normally evidenced by an exponentially increasing rate.

Henderson [10] stated that the oxidation rates of sulfides containing copper and/or iron were not affected by changes in the gas velocity over the sulfide up to moderate rates, when a large excess of oxygen was present. Henderson [11] stated that the amount of air supplied to the furnace affected the oxidation in two ways. When very little

air is available, the rate of growth of the oxidized layer is controlled by the amount of oxygen available for reaction and small variations in the air supply have a large effect on the roast. Increasing the amount of air to the furnace has a progressively smaller effect and a point is finally reached when oxidation is almost independent of the supply of additional air. The air velocity in the furnace has still, however, some slight effect on the amount of sulfide oxidized at any arbitrary time, from the beginning of the experiment.

THERMODYNAMICS

The chemical and physical properties of stibnite and the antimony oxides are given as follows: The melting points are 550°C for Sb_2S_3 and 656°C for Sb_2O_3, Sb_2O_4 and Sb_2O_5. The boiling point of Sb_2O_3 is 1550°C. The vapor pressures of Sb_2O_3 (after Kelley [12]) are shown in Table 7 Appendix I. At 930°C, Sb_2O_4 loses an oxygen atom and thus is dissociated into Sb_2O_3. Sb_2O_5 dissociates into Sb_2O_4 and an oxygen atom at 380°C.

The following reactions represent the three possible products of stibnite oxidation

$$Sb_2S_3 + 9/2O_2 = Sb_2O_3 + 3SO_2 \qquad \text{(I)}$$

$$Sb_2S_3 + 5O_2 = Sb_2O_4 + 3SO_2 \qquad \text{(II)}$$

$$Sb_2S_3 + 11/2O_2 = Sb_2O_5 + 3SO_2 \qquad \text{(III)}$$

The free energy changes of the reactions were calculated for various temperatures, ranging from 25°C to 900°C. The results of these calculations along with references to sources of data are tabulated in Tables 1 to 3 (Appendix I) and shown in Figure 3. The free energy of oxygen at temperatures other than 25°C was calculated using the relationship

$$\Delta F^\circ = \Delta H^\circ - T\Delta S^\circ$$

where $\Delta H^\circ = 8.27T + 1/2(0.258 \times 10^{-3})T^2 + \frac{1.877 \times 10^5}{T} - 3007$ [13]

and $\Delta S^\circ = 8.27 \ln T + (0.258 \times 10^{-3})T + \frac{1.877 \times 10^5}{2T^2} - 48.25$ [13]

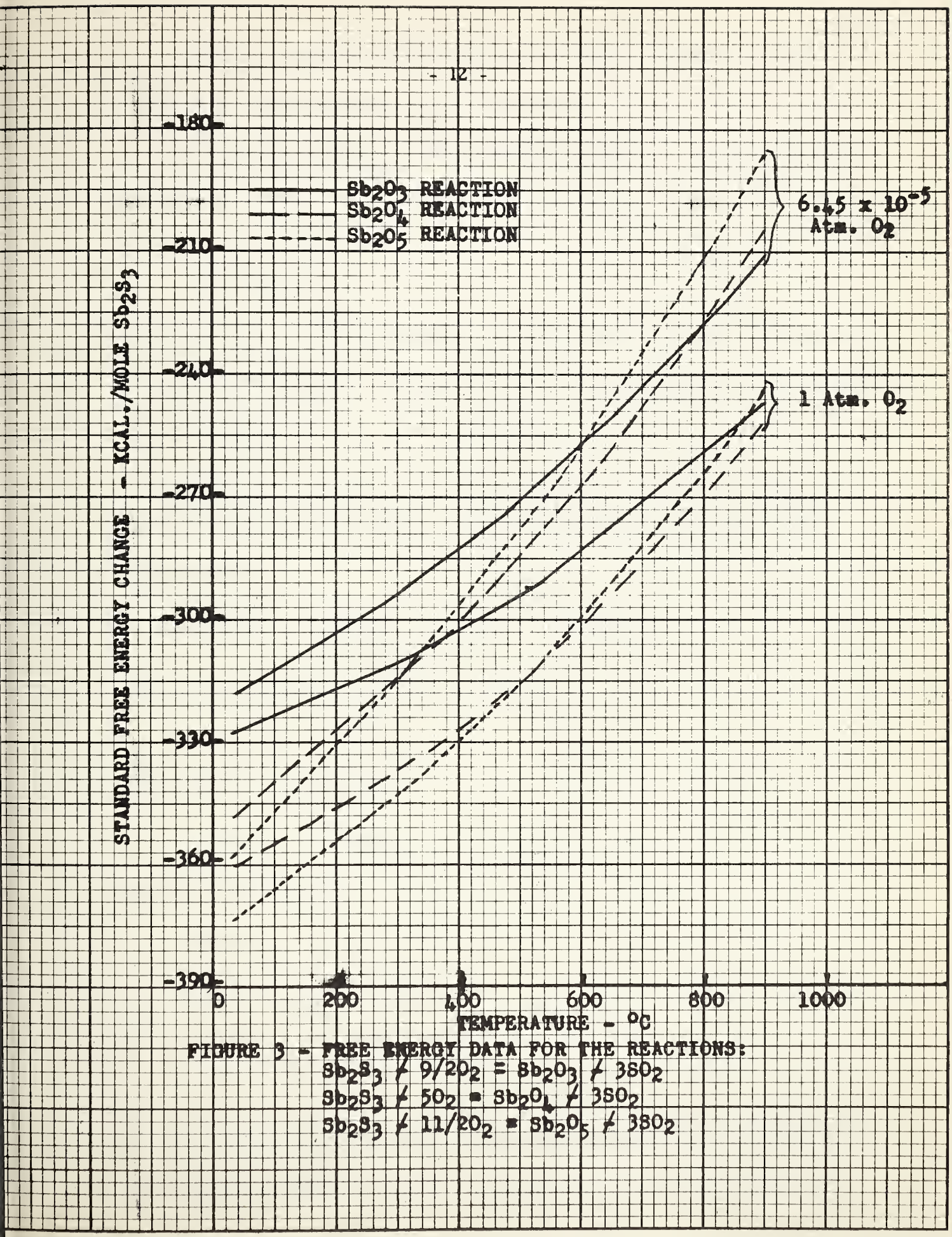

FIGURE 3 - FREE ENERGY DATA FOR THE REACTIONS:

$Sb_2S_3 + 9/2O_2 = Sb_2O_3 + 3SO_2$

$Sb_2S_3 + 5O_2 = Sb_2O_4 + 3SO_2$

$Sb_2S_3 + 11/2O_2 = Sb_2O_5 + 3SO_2$

Since a constant volume was maintained in experiments the number of moles of oxygen and sulfur dioxide was calculated from the stoichiometric equation for a given partial pressure of oxygen. Oxygen and sulfur dioxide were assumed to act as ideal gases and the following equation was used:

$$pV = nRT$$

Since the volume was constant the partial pressure of sulfur dioxide was found when the number of moles of sulfur dioxide was known. The number of moles per unit of volume changed as the temperature was varied but the partial pressures remained constant. If n moles of oxygen reacted with stibnite following reaction (I) the number of moles of SO_2 formed was:

$$n_{(SO_2)} = \frac{3 \times 64}{4.5 \times 32} \times n_{(O_2)} = 1.33 n_{(O_2)}$$

Therefore, in order to satisfy the gas law

$$P_{(SO_2)} = 1.33 p_{(O_2)}$$

Similarly for reaction (II)

$$P_{(SO_2)} = 1.20 p_{(O_2)}$$

and for reaction (III)

$$P_{(SO_2)} = 1.09 p_{(O_2)}$$

Thus, using the equation:

$$\Delta F = \Delta F^{o} + RT \ln \left(\frac{P_{(SO_2)}^{3}}{P_{(O_2)}^{n}} \right)$$

where n is the number of moles of oxygen reacting (in the stoichiometric equation). The changes in the free energies for the three reactions were

calculated for various partial pressures of oxygen. These values are tabulated in Tables 4 to 6 Appendix I and shown in Figure 3.

From these results the following conclusions can be drawn:

1. At one atmosphere oxygen pressure, reaction (III) is preferred from 25° to 500°C; reaction (II) is preferred from 550°C to 900°C and reaction (I) is the least preferred reaction between 25°C and 900°C.
2. At oxygen partial pressures of 0.35, 0.21 and 0.05 atmospheres, reaction (III) is preferred from 25°C to 400°C and reaction (II) is preferred from 500°C to 900°C.
3. At an oxygen partial pressure of 6.45×10^{-5} atmospheres, reaction (III) is preferred from 25°C to 300°C, reaction (II) is preferred from 400°C to 800°C and reaction (I) is preferred from 800°C to 900°C.

However it is possible for any of the three reactions to occur since the free energy change is negative in every case. The tendency of one of the reactions to occur in preference to the others would be based on activation energies since there is no great difference in the values of the free energy changes.

KINETICS

The rate of a reaction occurring at a solid-gas interface involves five stages: (1) Transport of the gaseous reactant to the surface;

(2) Adsorption of the gas; (3) Reaction at the surface; (4) Desorption of one or both products; and, (5) Transport of the desorbed products from the surface into the bulk gas phase. It is possible that any one of these stages may be rate determining. Activation energies, which can be calculated from an Arrhenius plot (ln Rate vs. $\frac{1}{T}$), are indicative of the stage which controls the overall rate of the reaction.

DIFFUSION (Stages 1 & 5)

In a gas-solid reaction the transport of the gaseous reactants to the surface and removal of the products from the surface to the bulk gas phase are ordinarily diffusion processes. If either one of these diffusion processes is the rate controlling mechanism, the value of the activation energy for the overall reaction will be very small or negligible (gaseous diffusion involves little or no activation energy). The rate of a process, when controlled by the diffusion rate of one component, can be expressed by Fick's first law, i.e.,

$$\vec{J} = D \frac{\partial c}{\partial x} \qquad (1)$$

Where $\vec{J}$ is the flux of the diffusing component, D is the diffusion coefficient (assumed constant) and $\frac{\partial c}{\partial x}$ is the concentration gradient.

If it is assumed that transport of the gaseous reactants i.e. oxygen, to the reacting surface through an impoverished film in the gas phase is the slow step, then the rate of reaction (I) is given by

$$\text{Rate } (SO_2 \text{production}) = \frac{d(SO_2)}{dt} = \frac{3}{4.5} D \frac{\partial c}{\partial x} \qquad (2)$$

where $\frac{\partial c}{\partial x}$ is the oxygen concentration gradient. For an impoverished gaseous film of thickness t, $\frac{\partial c}{\partial x}$ may be taken as $\frac{Co}{t}$, where Co is the original concentration of oxygen in the gas phase. For a given flow t is constant. The rate of SO_2 production is in the ratio 3/4.5 since for every 9/2 moles of O_2 reacting, 3 moles of SO_2 are formed.

Similarly, for reaction II the rate of SO_2 production is given by:

$$\text{Rate} = \frac{3}{5} D \frac{\partial c}{\partial x} \quad \ldots\ldots (3)$$

When steady state flow techniques are used, the most suitable form is that of expressing the reaction rates in terms of product formation, as in equations (2) and (3).

If stage (5) is the rate controlling mechanism, then the rate of reaction (SO_2 production) will be given by:

$$\text{Rate} = D \frac{\partial c}{\partial x} \quad \ldots\ldots (4)$$

where the concentration gradient is now that of SO_2.

It is possible, however, that the products forming on the surface, may remain there to form a retarding layer. In this case, the rate controlling mechanism would be diffusion of the reactant through the layer to the reacted material, which would involve solid diffusion and therefore a correspondingly higher activation energy. The expression for the rate would again be given by equation (2) or (3), with the modification that the thickness of the retarding layer, t, increases with time. This is probably the case in the present investigation since all

of the antimony oxides are solid at the temperatures and pressures investigated. However, if the layer is composed of Sb_2O_3, it will necessarily evaporate at some rate because the vapor pressure is probably less than the equilibrium pressure (10^{-4} atmos.) due to flow conditions.

ADSORPTION AND DESORPTION (Stages 2 & 4)

In many solid/gas reactions, adsorption of the reactant gas molecules onto the surface is a slow and therefore a rate determining step. The activation energies for adsorption approach those for chemical reactions but in general are smaller, of the order of 20 kcal./mole. The strength of the bond is indicated by the heat evolved on adsorption.

Adsorption of a gas molecule on a solid surface is often accompanied by a dissociation of the molecule. Two main types of behavior may be distinguished: (A) that in which the molecule undergoes dissociation in the course of adsorption but the atoms remain on adjacent sites; (B) that in which dissociation results from the jump of one or both of the atoms constituting the molecule from one site to another. Glasstone et al [19] have derived expressions for the rates of adsorption and desorption and the adsorption isotherms for these two cases. If the reaction is controlled by the adsorption rate of oxygen on the surface, i.e. the surface reaction and desorption of the products are both fast, then desorption of the reactants need not be considered. The reaction rates are then proportional to the adsorption rates of oxygen. For case (A) Glasstone derives the following adsorption rate:

$$V_1 = c_g c_s \frac{kT}{h} \cdot \frac{F^{\neq}}{F_g F_s} e^{-\epsilon_1/kT} \quad \ldots\ldots\ldots\ldots\ldots\ldots\ldots (5)$$

where V_1, is the rate of adsorption, c_g is the concentration of the gas, c_s represents the total number of bare sites per square centimeter, k is the Boltzman constant, T is the absolute temperature, h is the Planck constant, $f^{\neq}$ is the partition function of the activated complex which does not include the contribution due to translational motion, F_g is the partition function for unit volume of gas undergoing adsorption, f_s is the complete partition function of the solid, and ϵ_1 is the apparent energy of activation for adsorption per single molecule at absolute zero.

Two possibilities arise for case (B): adsorption of the molecule may be rapid and the jump of the atom to the neighboring site is slow, or the adsorption of the molecule may be the rate determining stage. If the rate determining step is adsorption then the adsorption rate is also given by equation (5) which is directly proportional to the gas pressure. If the rate determining step is the dissociation then the adsorption rate is given by:

$$V_1 = c_g^{\frac{1}{2}} c_s \frac{kT}{h} \cdot \frac{F^{\neq}}{F_g^{\frac{1}{2}} F_s} e^{-\epsilon_1/kT} \quad \ldots\ldots\ldots\ldots\ldots (6)$$

which is proportional to the square root of the gas pressure.

Since the product, antimony oxide, is a solid at test temperature, desorption of antimony oxide is eliminated. However, desorption of SO_2 may be rate controlling. If this were so, the reaction rate would vary with changes in oxygen pressure.

SURFACE REACTION (Stage 3)

If the surface reaction is the rate determining step, then the rate may be expressed by:

$$\frac{d\,(SO_2)}{dt} = k_1\,(O_2)^Z \quad \text{.................................} (7)$$

where k_1 is a specific rate constant and Z is the reaction order. An increase in the flow rate should have no effect on the reaction rate only in so far as dilution by SO_2 is diminished. The magnitude of the activation energy for these reactions is in the order of 20 to 100 kcal./mole.

DESCRIPTION OF APPARATUS

A schematic diagram of the furnace and auxiliary equipment used are shown in Figure 4. A zircon combustion tube, $1\frac{3}{4}$ inches inside diameter and 36 inches long, had its center section (one foot long) externally woundwith Kanthal strip. The windings were insulated with alumina cement and a refractory mortar and then wrapped with asbestos rope to prevent slippage. The furnace temperature was measured with a chromel-alumel thermocouple located inside the furnace tube approximately at the center of the wound section. The furnace temperature was controlled by this thermocouple operating through an automatic "Symplytrol" temperature controller. The power input to the winding was separately adjusted by means of a 2 kw. powerstat which was linked directly to the temperature controller. This arrangement controlled the temperature in the reaction zone within $\pm$ 2°C of the setting. Accurate temperature readings were made by switching the thermocouple leads to a type 3184D Tinsley potentiometer.

The combustion tube was enclosed by a two inch refractory, then one-half inch of vermiculite, and four inches of insulating firebrick, all held in a sheet steel box. The top and bottom of the insulated portion of the furnace were each covered with a one inch thickness of Atlasite (amosite asbestos fibre) blocks and a one-quarter inch thickness of asbestos sheet. The combustion tube had female standard joints sealed onto its ends. The flow and partial pressures of oxygen and nitrogen were controlled by regulators, flowmeters (rotameters) and a manometer. A quartz spring balance with an attached index fiber was set

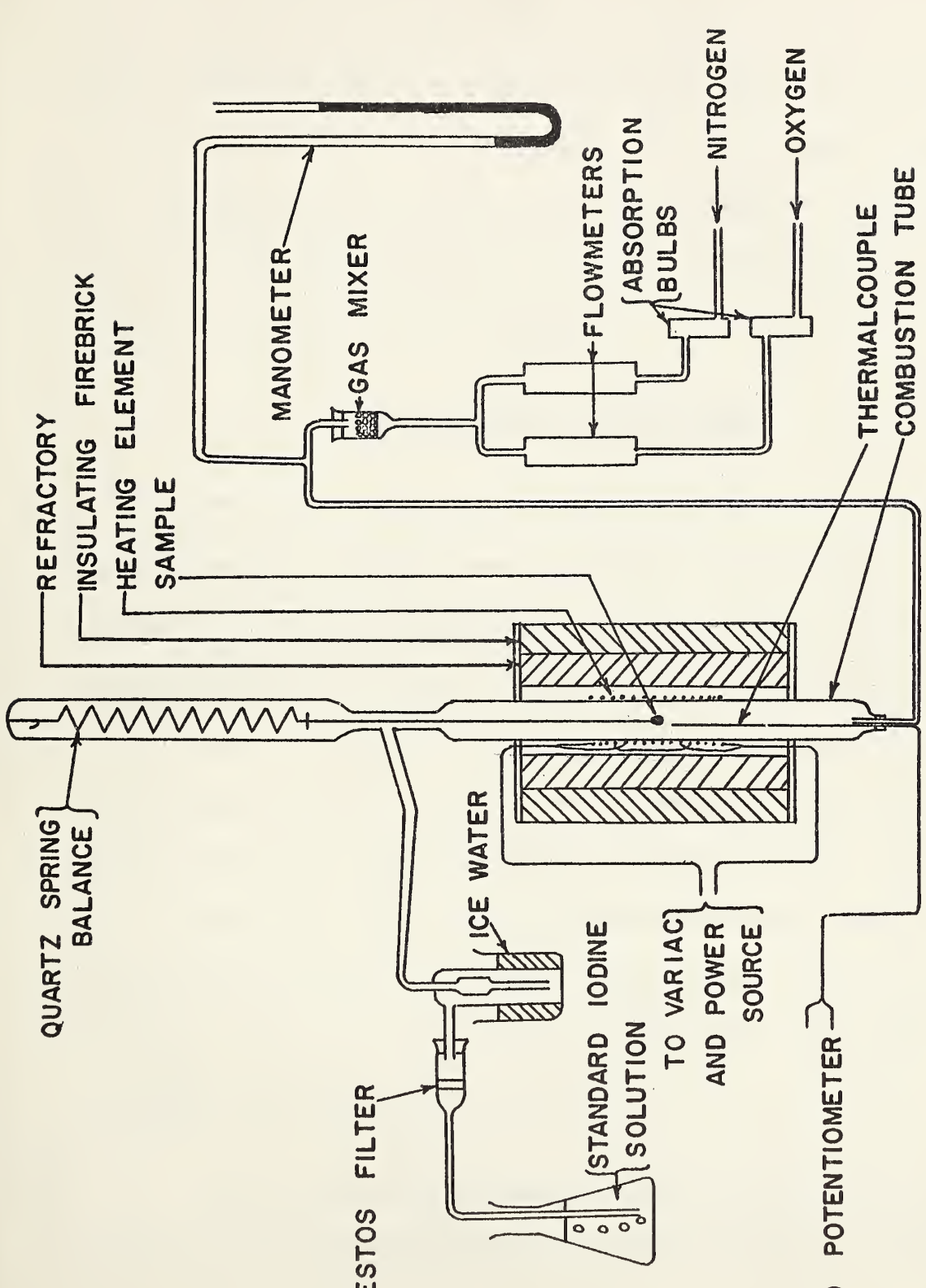

FIGURE 4- SCHEMATIC DIAGRAM OF VERTICAL TUBE FURNACE USED IN OXIDATION OF MINERALS

at the top of the combustion tube. A scale, divided into millimeters, and, mirror were placed directly behind the balance case and a "Misco" optical reader was mounted at forty-five degrees to the front of the case with its objective 40mm. from the index fiber. The scale and mirror could be read to $\pm$ 0.1 mm.(equivalent to $\pm$ 2 mg.in weight change). The roasting gases passed out of the furnace at the tee connection and then passed through the gas analysing train. This arrangement prevented the escape of the internal gases.

EXPERIMENTAL PROCEDURE

The stibnite used was a naturally occurring mineral in a multicrystalline form, obtained from Manhattan, Nevada, U.S.A. This was ground to a fine powder in a pestle and mortar. Three and one-half gram portions of this powder were pressed in a metallurgical press at 10,000 psi and 150°C for thirty minutes. The press was then allowed to cool slowly with the pressure being maintained. The briquets formed in this manner had an average thickness of 0.0641 inches. A small hole was drilled in each briquet which was suspended in the furnace with a platinum wire attached to the quartz spring balance. Surface areas (to $\pm$ 0.01 sq. ins.) of the briquets were determined by measuring areas from their photographs using a planimeter.

After the furnace was brought up to the required temperature, oxygen and nitrogen were introduced into the furnace at a regulated

constant flow rate and a constant partial pressure. After the system had been filled with gas the sample was introduced into the furnace. As the oxidation proceeded a rate curve was obtained by plotting weight changes vs. time. The product gases were bubbled through a standard iodine solution which was afterwards titrated with a standard sodium thiosulfate solution to determine the amount of SO_2 evolved. Another method of SO_2 determination would have been to bubble the gases through a solution in which the SO_2 would be changed to a sulfate. The sulfate would be precipitated as barium sulfate by adding barium chloride to this solution. The precipitate would be weighed and the amount of sulfur calculated.

A check-test to determine the amount of SO_3 formed and to find the SO_2 losses was conducted. A second flask of iodine was placed in the gas analyzing train. The pH of the iodine solution was taken at the start of the experiment with a pH meter. When the experiment was completed the iodine samples were divided. One-half was used for SO_2 determination with sodium thiosulfate while the other half was titrated with sodium hydroxide until the pH of the solution returned to the original value. The test showed that only two percent of the total amount of SO_2 evolved was collected in the second flask of iodine. Only a very slight amount of SO_3 was collected in the flasks. The method used for calculating the amount of SO_3 is shown in Appendix III. From these calculations it was found that a negligible amount of SO_3 was formed.

Tests were run keeping oxygen partial pressure and gas velocity constant and varying the temperature; keeping temperature and gas velocity constant and varying oxygen partial pressure; and keeping temperature and oxygen partial pressure constant and varying gas velocity.

For tests carried out above the melting point of stibnite (550°C) the procedure and apparatus were altered as follows: The reacting gases were introduced into the furnace at the tee connection at the top of the furnace and the product gases were removed from the bottom of the furnace. This allowed better contact of the reacting gases with the molten stibnite which was in a crucible suspended from the quartz spring balance. The furnace was brought to a temperature of 500°C and filled with nitrogen. The sample of ground stibnite in the crucible was then suspended in the reaction zone in the furnace and the temperature was raised to the required experimental temperature. The flow rates of oxygen and nitrogen were then adjusted to give the required partial pressure of oxygen at the required total gas flow rate.

In order to determine whether the platinum wire acted as a catalyst in the oxide formation on the sample, tests were conducted in which the sample was suspended with a quartz fiber instead of platinum wire. When the quartz fiber was used the same results were obtained as when the platinum wire was used. Thus it was concluded that the platinum wire used in suspending the sample in the furnace did not act as a cata-

lyst in the formation of the antimony oxide. Quartz fiber was not used in all the experiments because it is very brittle, and liable to cause the loss of the sample in the furnace.

EXPERIMENTAL RESULTS

The results are based on the oxidation of fifty-eight stibnite samples in the temperature range 300° to 750°C, at oxygen partial pressures varying from 35 to 245 mm.Hg, and with low gas flows (from 5 to 50 ml./min). In addition, one set of experiments was conducted at an oxygen partial pressure of 0.05 mm. of Hg and at a gas flow rate of 18,600 ml./min. Typical rate curves obtained experimentally are presented in Figures 5 and 6.

The volumes of SO_2 that were produced during an experiment were calculated using the method set forth by the Aluminum Company of Canada [15]. Using stoichiometry the weight of stibnite that had been oxidized was calculated from the volume of sulfur dioxide produced. Similarly, the amount of antimony trioxide that could be formed if all of the stibnite was oxidized to antimony trioxide was calculated. Similarly, the amount of antimony tetraoxide and the amount of antimony pentoxide that could be formed if all of the oxidized stibnite was antimony tetraoxide or antimony pentoxide respectively were calculated. For the purpose of these calculations it was assumed that all of the antimony oxide produced remained on the sample. Thus the weight

difference between the amount of stibnite oxidized and the amount of antimony oxide formed gave the theoretical sample weight loss. A sample calculation of this type is shown in Appendix IV. The results of these calculations are shown in Table 8 Appendix IV.

The rate of sulfur dioxide production per square centimeter of sample area was calculated. The results of these calculations are shown in Table 9 Appendix IV. Plots of some of these rates of sulfur dioxide formation vs. oxygen concentration are shown in Figure 7. An Arrhenius plot of $\log_e$ (Rate of SO_2 Formation) vs. the reciprocal of the absolute temperature is shown in Figure 8.

An attempt was made to collect the gaseous antimony trioxide in the trap shown in Figure 4 but very little antimony trioxide was collected in this manner. Most of the oxide precipitated on the walls of the furnace and auxiliary equipment.

At lower temperatures (300° and 350°C) no oxide film was observed on the sample after roasting had taken place. However, an oxide layer was observed at higher temperatures (400° and 450°C). In roasting tests made at temperatures above the melting point of stibnite (550°C) an oxide layer was observed on samples having been oxidized at 560° and 600°C while no oxide layer was observed on samples which were oxidized at temperatures above 600°C. The oxide that was formed on the sample was found to be soluble in tartaric acid and had a white color which indicated that it was either antimony trioxide or antimony

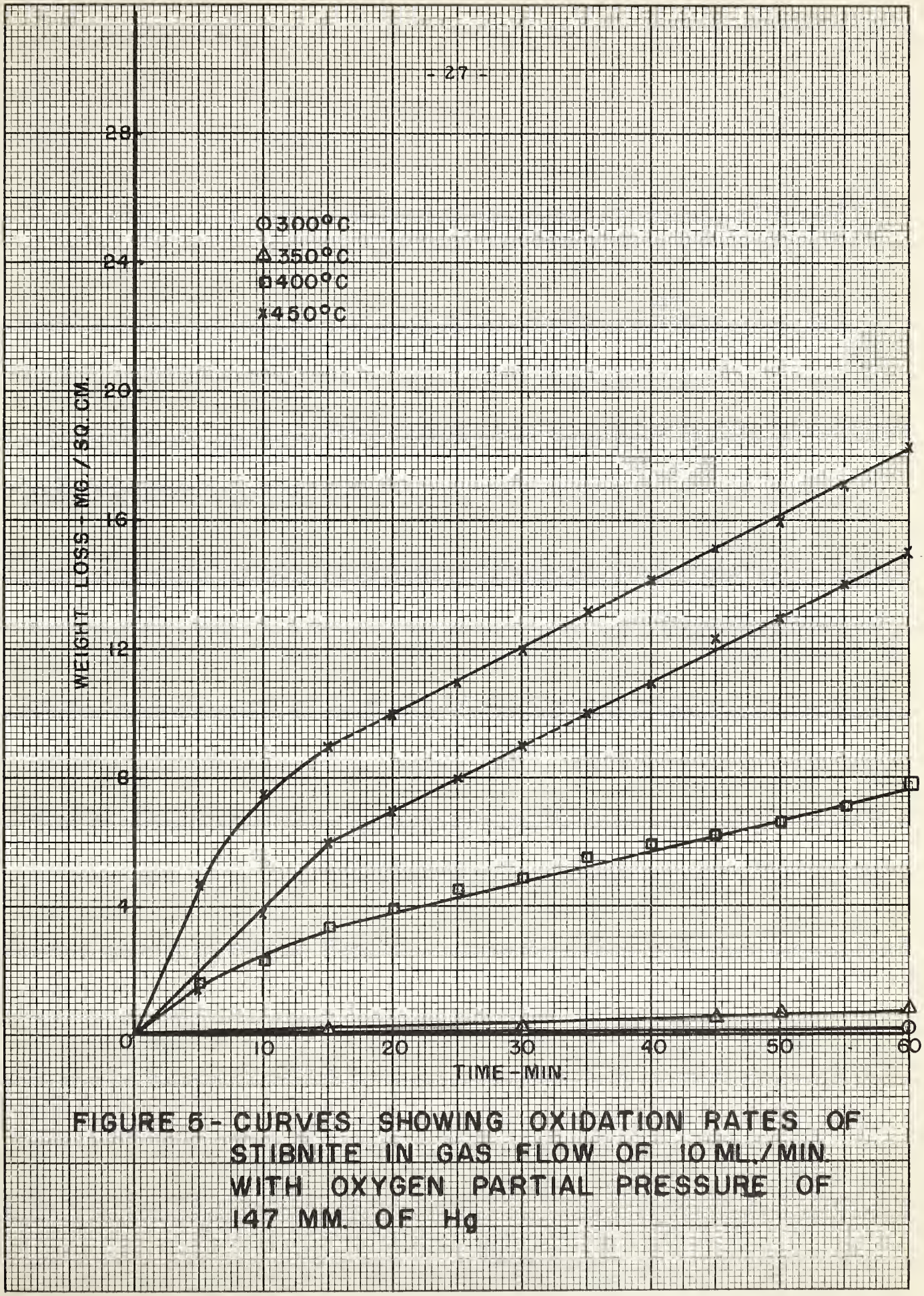

FIGURE 6 - CURVES SHOWING OXIDATION RATES OF STIBNITE IN GAS FLOW OF 10 ML./MIN. WITH OXYGEN PARTIAL PRESSURE OF 147 MM. OF Hg

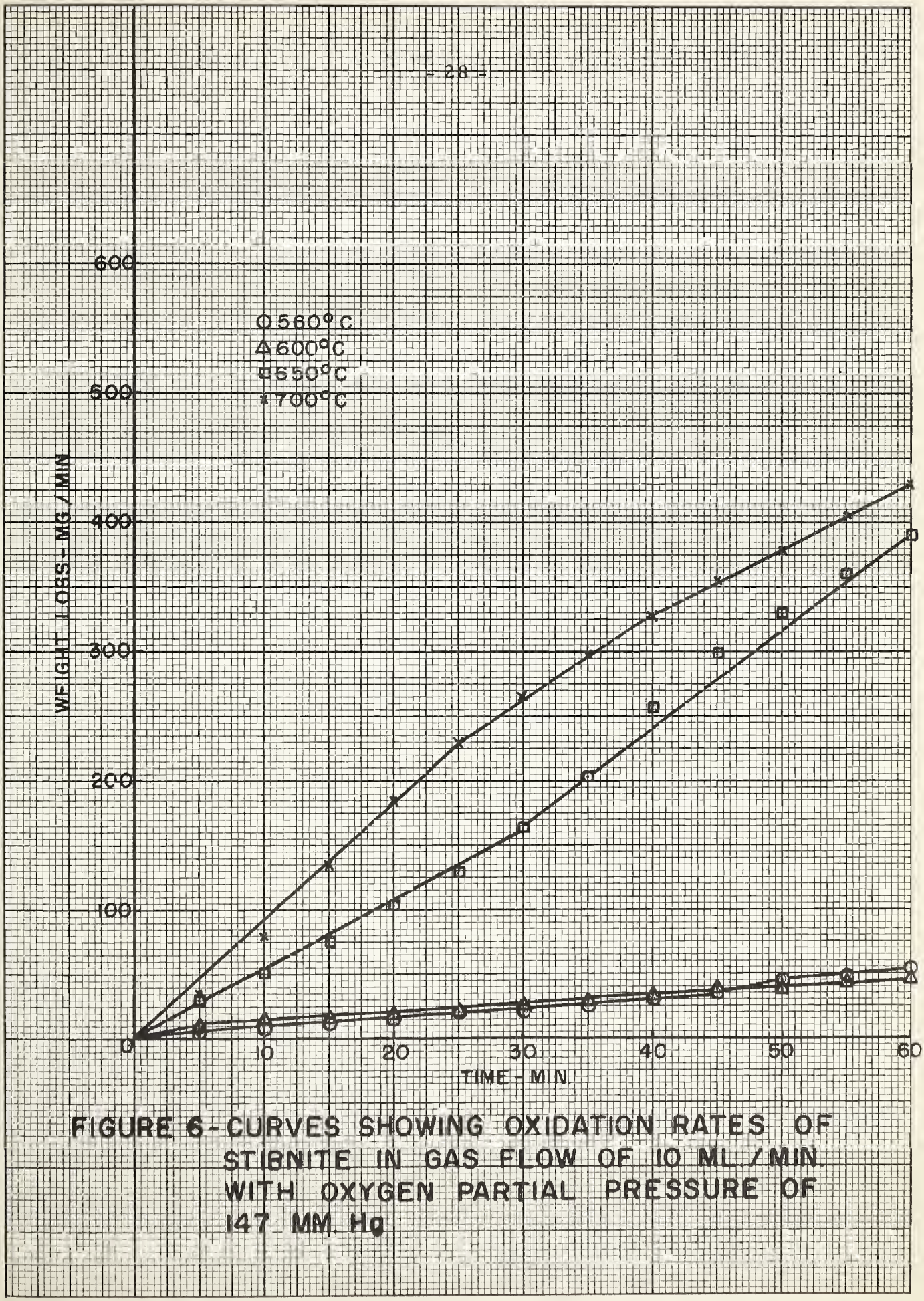

FIGURE 6 - CURVES SHOWING OXIDATION RATES OF STIBNITE IN GAS FLOW OF 10 ML / MIN WITH OXYGEN PARTIAL PRESSURE OF 147 MM Hg

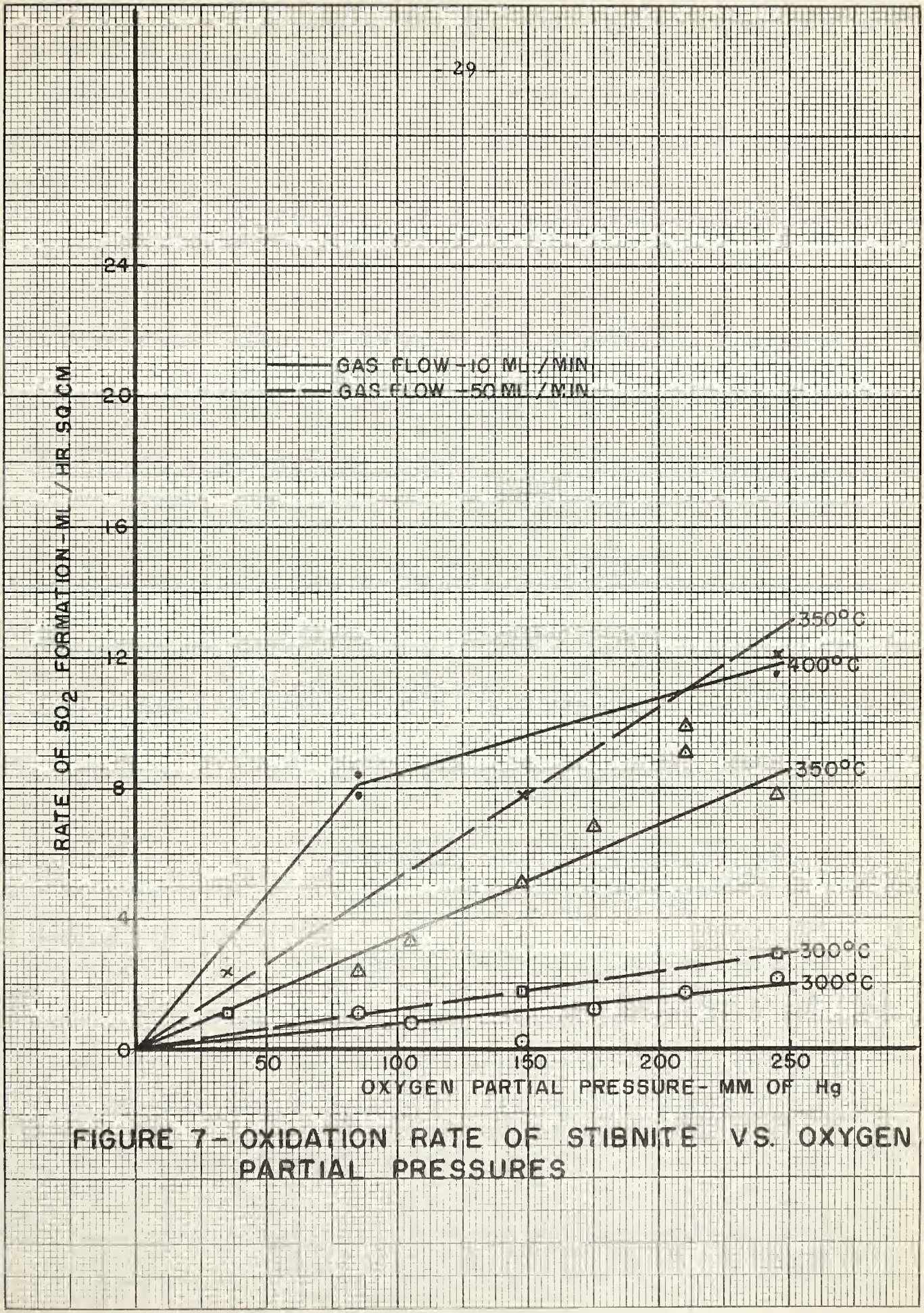

FIGURE 7 - OXIDATION RATE OF STIBNITE VS. OXYGEN PARTIAL PRESSURES

tetraoxide. Antimony pentoxide has a yellow color and is not soluble in tartaric acid [18]. Figure 9 shows a fresh stibnite sample (I) and one which has an oxide layer on it (II).

DISCUSSION OF RESULTS

A thermodynamical study of the stibnite-oxygen system suggests that the following reactions are possible:

$$Sb_2S_3 + 9/2O_2 = Sb_2O_3 + 3SO_2 \quad \text{(I)}$$

$$2Sb_2O_3 + O_2 = 2Sb_2O_4 = Sb_2O_3 \cdot Sb_2O_5 \quad \text{(II)}$$

$$\text{or } Sb_2S_3 + 5O_2 = Sb_2O_4 + 3SO_2 \quad \text{(II)}$$

$$Sb_2S_3 + 11/2O_2 = Sb_2O_5 + 3SO_2 \quad \text{(III)}$$

$$SO_2 + 1/2O_2 = SO_3 \quad \text{(IV)}$$

Of the above reactions, (III) and (IV) do not occur as found experimentally. Of the remaining, the tendency of one of the reactions to occur in preference to another would be determined by the magnitude of the activation energy.

It was found that the antimony trioxide was not removed from the system as a gas but deposited as a solid inside the furnace. This would be expected from studying the vapor pressure data, Table 7, and the chemical and physical properties of the antimony oxides. However, this is contrary to some present ideas [21] [23].

Since the stibnite briquets were made from a ground powder, the

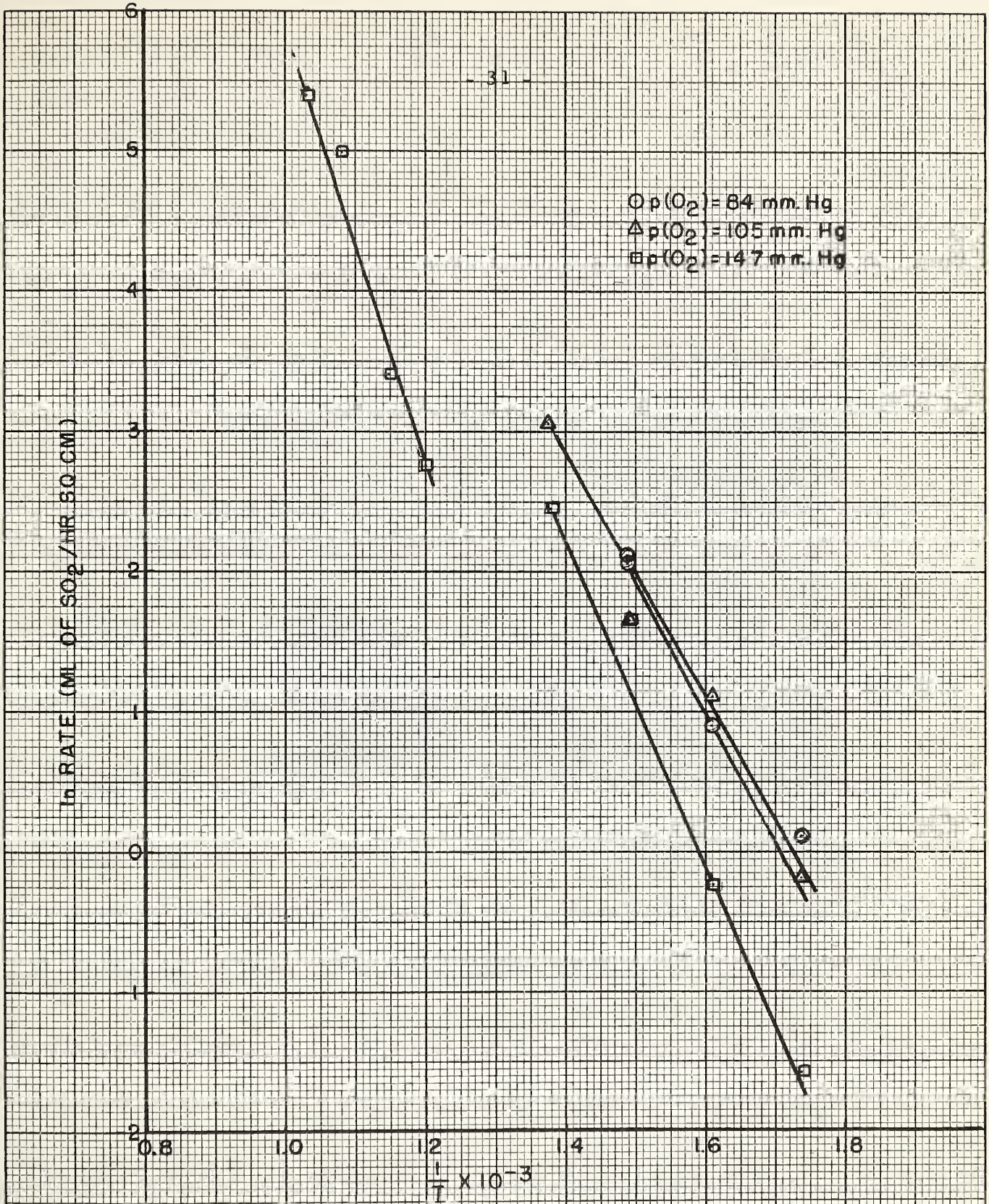

FIGURE 8 - ARRHENIUS PLOT SHOWING EXPERIMENTAL OXIDATION RATES OF STIBNITE IN A GAS FLOW OF 10 ML./MIN.

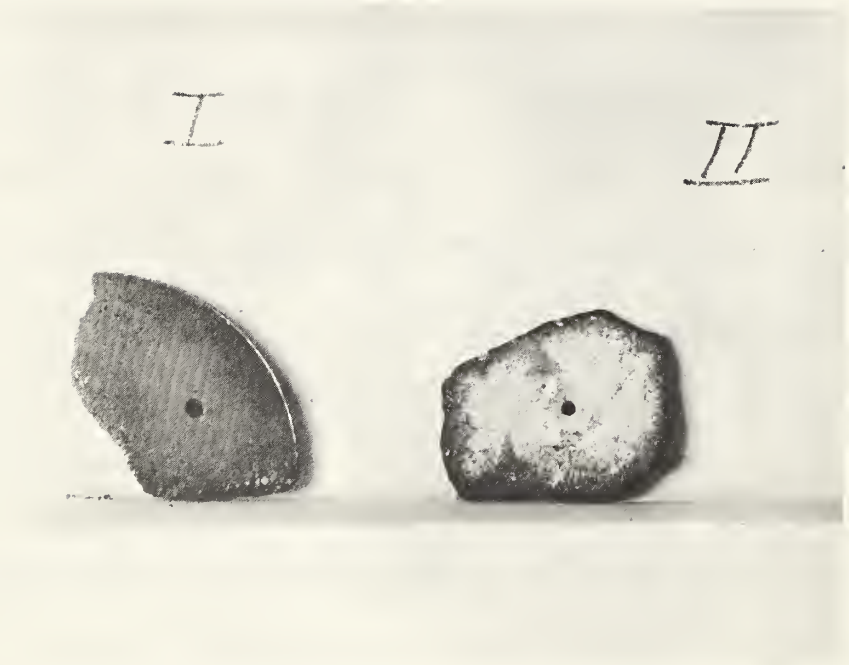

Figure 9 I - Fresh Stibnite Briquet

II - Stibnite Briquet Coated with Oxide layer

rates obtained are the average ones. The effect of different crystal faces can not be taken into account.

It was originally intended to calculate reaction rates from sample weight loss vs. time determinations. However, during the tests it was observed that antimony oxide was depositing on the furnace walls and on the sample itself. This made it impossible to determine the exact amount of Sb_2S_3 oxidized (as shown in Table 8), since that proportion of the antimony oxide deposited on the furnace walls and on the sample could not be calculated exactly. Therefore, sulfur dioxide yield is used in the determination of the reaction rates. Some useful information can however be determined from the weight loss vs. time curves and will be described later.

A slight error is introduced in the rate determination when using SO_2 results, since only one analysis for SO_2 was made for each test, and that at the completion of the one hour test. All of the weight loss vs. time curves for the temperature range of 300° to 500°C (Figure 5 is typical of these) show a constant rate after the first short time interval of five minutes. It is estimated that a maximum determinate error of plus 4% in the rate occurs if the rate of sulfur dioxide is taken as being constant over the entire experimental time of one hour. There is also present a determinate error of minus 2% in rate determination resulting from incomplete reaction of SO_2 with iodine in the gas analysis. Random errors due to pipetting and titration were very small in the

order of ± 1%.

A further positive determinate error in rate determinations must be considered. In Figure 5, the 450°C curves, as well as some SO_2 rates given in Table 9 show rather large discrepancies. This was due to the edge effects of the samples. It was found that under identical conditions, the sample with the greater edge length per unit of area oxidized more rapidly than that with less edge length per unit of area. The edges are more rapidly oxidized because of the higher surface free energy at an edge than at a face of the sample. Calculations were carried out which showed that at low and high temperatures a maximum of 5% and 10% respectively of the oxidation took place on the edge.

Another error which was introduced into these experiments was that the gas expanded in the furnace and thus a true flow rate was not shown and also the flow rate increased as the temperature increased. For a temperature increase from 300°C to 500°C the flow would increase by a factor of 1.3. However, an increase of flow of 5 times only doubled the rate of the reaction so that the effect of this error on the results would be very small.

Consideration of all the errors, experimental and graphical, shows that there is a systematic positive error of approximately 5% when the SO_2 determinations were used to determine the overall rate of the reaction for the tests run at 300° and 350°C.

Figure 7 shows a straight line relationship between the rate of sulfur dioxide production and the partial pressure of oxygen at temperatures of 300°C and 350°C. It also shows that the rate increased with an increase in gas flow. From Figure 7, the following relationships are deduced:

For the 300°C curve at a flow rate of 10 ml./min.

$$\frac{\text{Rate 1}}{\text{Rate 2}} = 1.06 \frac{p_1}{p_2}$$

where p_1 and p_2 are the partial pressures of oxygen corresponding to rates 1 and 2, corresponding to equations (I) and (II).

For the 350°C curve at a flow rate of 10 ml./min.

$$\frac{\text{Rate 1}}{\text{Rate 2}} = 1.02 \frac{p_1}{p_2}$$

For the 300°C curve at a flow rate of 50ml./min.

$$\frac{\text{Rate 1}}{\text{Rate 2}} = 1.09 \frac{p_1}{p_2}$$

For the 350°C curve at a flow rate of 50ml./min.

$$\frac{\text{Rate 1}}{\text{Rate 2}} = 1.02 \frac{p_1}{p_2}$$

It may be concluded, therefore, that the reaction rates at 300°C and 350°C are directly proportional to oxygen pressure.

The above results, suggest one of two possible rate controlling mechanisms: gaseous diffusion or adsorption, since the proportionality of rate to oxygen pressure is given by equations (2), (3) and (5). The dissociation step in adsorption cannot be rate determining since this would involve a square root dependency of rate with oxygen partial pres-

sure (equation 6). Both the rate of gaseous diffusion and the rate of adsorption are increased as the rate of flow of the gas is increased. In the case of gaseous diffusion the increased reaction rate with increased flow rate could be due to a decrease in the thickness of the oxygen impoverished film. If adsorption is the rate determining step, then the increase in reaction rate with increased flow rate could be the result of diminished dilution resulting from the SO_2 evolution.

The activation energy for the process was calculated from the slopes of the best fit lines of the Arrhenius plots shown in Figure 8. The experimental activation energies, from Figure 8, were 18.3 kcal./mole, 18.2 kcal./mole, and 22.4 kcal./mole for partial pressures of oxygen of 84 mm.of Hg, 105 mm.of Hg, and 147 mm.of Hg respectively. The gas flow in each of these cases was 10 ml./min. As might be expected, it would appear that gaseous diffusion as a rate determining step is eliminated considering the magnitude of the activation energies. Diffusion through a solid layer on the sample as the rate determining step is also excluded since this would involve an increase in layer thickness with time and therefore a corresponding decrease in rate. This is not observed in the rate vs. oxygen pressure curves (Figure 7) or in the weight loss vs. time curves (Figure 5) (as indicated by the linearity of the curves). Therefore it is more probable that adsorption is the rate controlling mechanism for the temperature range 300°C to 350°C.

The initial rapid rate of the reaction, shown in Figure 5 and in the other weight loss vs. time curves, may be attributed to adsorption of oxygen from the atmosphere on the sample prior to the test. Since the surface reaction is fast, this adsorbed oxygen would react immediately and give the higher reaction rates observed during the initial stages of the test.

The 400°C curve shown in Figure 7 does not follow the relationship

$$\frac{\text{Rate 1}}{\text{Rate 2}} = \frac{P_1}{P_2}$$

but slows down considerably. This curve shows that possibly the rate controlling mechanism was the diffusion of oxygen through the layer of oxide formed on the sample. This is quite probable at the higher temperature since there would be a higher deposition rate of antimony oxide on the surface of the sample. In this case the rate would not be directly proportional to the oxygen partial pressure. However, the activation energy for diffusion through a porous solid could be of the order of 20 kcal./mole.

For molten stibnite the experimental activation energy obtained was 31.6 kcal./mole for a partial pressure of oxygen of 147 mm. of Hg in a gas flow of 10 ml./min. The magnitude of the activation energy would suggest a more difficult adsorption process or that surface reaction is the rate determining step.

CONCLUSIONS

The antimony oxide formed during the oxidation of stibnite is either antimony trioxide, or antimony tetraoxide or both. These are both solids and are not removed from the sphere of roasting.

The rate of the oxidation of stibnite is controlled by two or possibly three processes between 300°C and 700°C. At low temperatures (300°C to 350°C) the reaction rate is controlled by adsorption of oxygen onto the solid. From 400°C to 500°C the rate determining step is probably diffusion of the oxygen through a porous layer of antimony oxide on the sample. Above the melting point of stibnite (550°C) the rate determining process could be either adsorption of the oxygen or the reaction at the surface.

The activation energy for the oxidation of stibnite below and above its melting point is of the order of 20 and 30 kcal./mole respectively.

The main object of this work was to determine the conditions in which the roasting of stibnite could be carried out with removal of the roasting products as gases. In the temperature range, 650°C to 700°C the products were removed from the sample as gases at an appreciable rate but the antimony oxide precipitated in the furnace. This would not be a practical method of removing the antimony unless some method or apparatus was designed to completely remove the antimony from the furnace.

The furnace design was found to be quite adequate for the tests described in this work and no changes would be necessary to carry out further experiments.

Suggested changes in procedure for any further work to be carried out are to devise some method of coating the edges of the samples in order to eliminate the discrepancies due to the edge effects and to adjust the procedure so that SO_2 determinations can be made during roasting.

BIBLIOGRAPHY

1. Cazafura, K., "Chemistry of Roasting Arsenic Trisulfide, Antimony Trisulfide, Cobalt Sulfide and Nickel Sulfide, As Well As, Their Binary Mixtures", Rudarsko - Metalurski Zbornik, Ljubljana, 1957, No. 4, Pages 345 to 361.

2. Charrier, J., "Study of the Decomposition of Sulfides by Means of Thermogravimetric Analysis", Bull. soc. hist. nat., Toulouse, Vol. 85, 1950, Pages 317 to 330.

3. Kellogg, H.H., "Equilibrium Considerations in the Roasting of Metallic Sulfides", Journal of Metals, Vol. 8, 1956 Pages 1105 to 1111.

4. Dannatt, C.W., and Ellingham, H.J.T., "Roasting and Reduction Processes - A General Survey", Faraday Society Discussions, No. 4, 1948, Pages 126 to 139.

5. Peretti, E A., "A New Method For Studying The Mechanism Of Roasting Reactions", Faraday Society Discussions, No. 4, 1948, Pages 174 to 179.

6. Polyvyanni, I.R., "Dependence of Oxidation Rate on the Nature of Sulfides", Izvest. Akad. Nauk Kazakh. S.S R., Ser. Gorhogo Dela, Met., Stroitel i Stroimaterialov, Vol. 4, 1957, Pages 84 to 96.

7. Diev, N.P., Okunev, A.I., Paduchev, V.V., Toropova, V.V., and Mokronosov, V.S., "Sulfur Monoxide As An Intermediate

Oxidation Product of Some Sulfides", Doklady Akad. Nauk S.S.S.R., Vol. 107, 1956, Pages 273 to 275.

8. Thornhill, P.G., And Pidgeon, L.M., "Micrographic Study Of Sulfide Roasting", Journal of Metals, Vol. 9, 1957, Pages 989 to 995.

9. Ong, J.N., Wadsworth, M.E., and Fassel, Jr., W.M., "Kinetic Study of the Oxidation of Sphalerite", Journal of Metals, Vol. 8, No. 2, 1956, Pages 257 to 263.

10. Henderson, T.A., "The Oxidation Rates of Lump Copper - Iron Sulfides", Trans. I.M.M., Vol. 67, 1957-58, Pages 437 to 462.

11. Henderson, T.A., "The Oxidation of Powder Compacts of Copper-Iron Sulfides", Trans. I.M.M., Vol, 67, 1957-58, Pages 497 to 520.

12. Kelley K.K., "Contributions to the Data on Theoretical Metallurgy III The Free Energies of Vaporization and Vapor Pressures of Inorganic Substances", U.S. Bureau of Mines, Bulletin 383, Page 110.

13. Rossini, F.D., Wagman, D.D., Evans, W.H., Levine, S., and Jaffe, I., "Selected Values of Chemical Thermodynamic Properties", U.S. National Bureau of Standards, Circular 500, Pages 90 to 94 and 582 to 583.

14. Wada, T., And Niwa, K., "A Kinetic Study on the Oxidation of Zinc Sulfide", Journal of Science, Hokkaido University , Series 3, Chemistry Vol. 5, No. 1, 1957, Pages 8 to 16.

15. "Methods of Chemical Analysis" - Aluminum Laboratories Limited, Arvida.

16. Coughlin, J.P., "Contributions to the Data on Theoretical Metallurgy XII Heats and Free Energies of Formation of Inorganic Oxides", U.S. Bureau of Mines, Bulletin 542, Pages 7 to 10 and 48.

17. Bailey, A.R., "A Text-Book of Metallurgy", MacMillan & Co. Ltd., London, 1960, Page 233

18. "Handbook of Chemistry and Physics" 37th Edition, Chemical Rubber Publishing Co., Cleveland, Ohio, 1955-1956, Pages 476 and 477.

19. Glasstone, S., Laidler, K.J., and Eyring, H.J., "The Theory of Rate Processes", McGraw-Hill Book Company, Inc., New York, 1941, Pages 369 to 392 and 519.

20. Millard, E.B., "Physical Chemistry For Colleges", McGraw-Hill Book Company, Inc., New York, 1953, Pages 425 to 457.

21. McClelland, W.R., "Laboratory Tests and Milling Practice on British Columbia Gold Ores", Trans. C.I M.M., Vol. XL, 1937,

pages 71 to 73.

22. Carter, R. and Samis, C.S., "The Influence of Roasting Temperature Upon Gold Extraction by Cyanidation from Refractory Gold Ores", Trans. C.I.M.M., Vol. LV, 1952, page 126.

23. Archibald, F.R., Martin, F.J. and Koenen, A.T., "Roasting of Beattie Concentrate", Trans. C.I M.M. Vol. XLII, 1939 page 625.

24. Kolthoff, I.M. and Sandell, E.B., "Textbook of Quantitative Inorganic Analysis", The MacMillan Company, New York, 1947, Page 329.

APPENDIX I

THERMODYNAMIC CALCULATIONS

Table 1 - Free Energies at Various Temperatures for the Reaction $Sb_2S_3 + 9/2O_2 = Sb_2O_3 + 3\,SO_2$.

Temp. °C	Temp. °K	(A) $\Delta F°$ $3SO_2$ (16) Kcal./mole Sb_2O_3	(B) $\Delta F°$ Sb_2O_3 (16) Kcal./mole Sb_2O_3	(C) $\Delta F°$ Sb_2S_3 (17) Kcal./mole Sb_2O_3	(D) $\Delta F°$ $9/2\,O_2$ (13) Kcal./mole Sb_2O_3	$\Delta F°$ Reaction A+B-C-D Kcal./mole Sb_2O_3
25	298	-243.9	-149.1	-65.1	0	-327.9
300	573	-229.6	-131.4	-47.8	- 2.7	-310.5
350	623	-227.0	-128.3	-44.7	- 3.6	-307.0
400	673	-224.4	-125.2	-41.7	- 5.4	-302.5
450	723	-221.8	-122.1	-38.8	- 6.7	-298.4
500	773	-219.1	-119.0	-36.0	- 8.1	-294.0
550	823	-216.5	-115.9	-33.8	- 9.9	-288.7
600	873	-213.8	-112.8	-32.3	-10.8	-283.5
650	923	-211.2	-109.8	-30.8	-13.5	-276.7
700	973	-208.6	-106.8	-29.3	-15.3	-270.8
750	1023	-206.0	-104.0	-27.7	-17.1	-265.2
800	1073	-203.4	-101.3	-26.0	-19.3	-259.4
900	1173	-198.1	- 95.9	-23.1	-26.1	-244.8

Table 2 - Free Energies at Various Temperatures For the Reaction $Sb_2S_3 + 5\ O_2 = Sb_2O_4 + 3\ SO_2$

Temp. °C	Temp. °K	(A)$\Delta F°$ $3SO_2$(16) Kcal./mole Sb_2O_4	(B)$\Delta F°$ Sb_2O_4(16) Kcal./mole Sb_2O_4	(C)$\Delta F°$ Sb_2S_3(17) Kcal./mole Sb_2O_4	(D)$\Delta F°$ $5\ O_2$(13) Kcal./mole Sb_2O_4	$\Delta F°$ Reaction A+B-C-D Kcal./mole Sb_2O_4
25	298	-243.9	-182.5	-65.1	0	-361.3
300	573	-229.6	-158.3	-47.8	- 3.0	-337.1
350	623	-227.0	-154.0	-44.7	- 4.0	-332.3
400	673	-224.4	-149.8	-41.7	- 6.0	-326.5
450	723	-221.8	-145.4	-38.8	- 7.5	-320.9
500	773	-219.1	-140.9	-36.0	- 9.0	-315.0
550	823	-216.5	-136.5	-33.8	-11.0	-308.2
600	873	-213.8	-132.3	-32.3	-12.0	-301.8
650	923	-211.2	-127.8	-30.8	-15.0	-293.2
700	973	-208.6	-123.1	-29.3	-17.0	-285.4
750	1023	-206.0	-118.4	-27.7	-19.0	-277.7
800	1073	-203.4	-113.9	-26.0	-21.5	-269.8
900	1173	-198.1	-104.6	-23.1	-29.0	-250.6

Table 3 - Free Energies At Various Temperatures For the Reaction $Sb_2S_3 + 11/2\ O_2 = Sb_2O_5 + 3\ SO_2$

Temp. °C	Temp. °K	(A) Δ F° $3SO_2$ (16) Kcal./mole Sb_2O_5	(B) Δ F° Sb_2O_5 (16) Kcal./mole Sb_2O_5	(C) Δ F° Sb_2S_3 (17) Kcal./mole Sb_2O_5	(D) Δ F° $11/2O_2$ (13) Kcal./mole Sb_2O_5	Δ F° Reaction A+B-C-D Kcal./mole Sb_2O_5
25	298	-243.9	-195.5	-65.1	0	-374.3
300	573	-229.6	-164.5	-47.8	- 3.3	-343.0
350	623	-227.0	-159.0	-44.7	- 4.4	-336.9
400	673	-224.4	-153.5	-41.7	- 6.6	-329.6
450	723	-221.8	-148.0	-38.8	- 8.2	-322.8
500	773	-220.1	-142.5	-36.0	- 9.9	-316.7
550	823	-216.5	-137.1	-33.8	-12.1	-307.7
600	873	-213.8	-131.8	-32.3	-13.2	-300.1
650	923	-211.2	-126.5	-30.8	-16.5	-290.4
700	973	-208.6	-121.0	-29.3	-18.7	-281.6
750	1023	-206.0	-115.5	-27.7	-20.9	-272.9
800	1073	-203.4	-110.0	-26.0	-23.6	-263.8
900	1173	-198.1	- 99.3	-23.1	-31.9	-242.4

Table 4 - Free Energies in Kcal./mole of Sb_2O_3 at Various Temperatures and Oxygen Partial Pressures for the Reaction $Sb_2S_3 + 9/2O_2 = Sb_2O_3 + 3SO_2$

Temp. °C	Temp. °K / $p(O_2)$ atm.	6.45×10^{-5}	0.05	0.21	0.35
25	298	-318.9	-324.7	-326.0	-326.5
300	573	-293.2	-304.4	-306.9	-307.7
400	673	-282.1	-295.3	-298.2	-299.3
500	773	-270.6	-285.8	-289.1	-290.3
550	823	-263.8	-280.0	-283.5	-284.7
600	873	-257.1	-274.2	-277.9	-279.3
700	973	-241.4	-260.5	-264.6	-266.1
800	1073	-227.0	-248.0	-252.6	-254.2
900	1173	-210.4	-233.3	-238.3	-240.2

Table 5 - Free Energies in Kcal./mole of Sb_2O_4 at Various Temperatures and Oxygen Partial Pressures for the Reaction $Sb_2S_3 + 5\ O_2 = Sb_2O_4 + 3\ SO_2$

Temp. °C	Temp. °K / $p(O_2)$ atm.	6.45×10^{-5}	0.05	0.21	0.35
25	298	-349.4	-357.3	-359.0	-359.6
300	573	-314.3	-329.3	-332.6	-333.7
400	673	-300.7	-318.4	-322.2	-323.5
500	773	-284.2	-304.5	-308.9	-310.5
550	823	-275.4	-297.0	-301.7	-303.4
600	873	-267.0	-290.0	-294.9	-296.7
700	973	-246.6	-272.2	-277.7	-279.7
800	1073	-227.0	-255.3	-261.4	-263.5
900	1173	-203.8	-234.7	-241.4	-243.7

Table 6 - Free Energies in Kcal./mole of Sb_2O_5 at Various Temperatures And Oxygen Partial Pressures For The Reaction $Sb_2S_3 + 11/2O_2 = Sb_2O_5 + 3\ SO_2$

Temp. °C	Temp. °K	p(O_2) atm. 6.45×10^{-5}	0.05	0.21	0.35
25	298	-359.5	-369.4	-371.6	-372.3
300	573	-314.6	-333.5	-337.7	-339.1
400	673	-296.3	-318.5	-323.4	-325.0
500	773	-277.5	-302.9	-308.6	-310.4
550	823	-266.9	-294.1	-300.1	-302.1
600	873	-256.9	-285.7	-292.1	-294.1
700	973	-233.5	-265.5	-272.7	-274.8
800	1073	-210.7	-246.1	-253.9	-256.4
900	1173	-184.4	-223.0	-231.6	-234.3

Table 7 - Vapor Pressures of Sb_2O_3 After Kelley [12]

Temperature °C	Temperature °K	Vapor Pressure Atmospheres
505	778	0.0001
568	841	0.001
647	920	0.01
910	1183	0.1
1073	1346	0.25
1228	1501	0.5
1425	1698	1.0

APPENDIX II

FURNACE CONSTRUCTION DETAILS

A. Furnace Winding

The furnace was wound in two sections in order to try to eliminate a temperature gradient in the reaction zone. A slight gradient still remained but its effect was only noticeable at the extreme ends of the wound portion of the furnace. Figure 10 shows the arrangement of the furnace windings.

B. Temperature Controller and Powerstat

Figure 11 shows the wiring diagram for the temperature controller and powerstat.

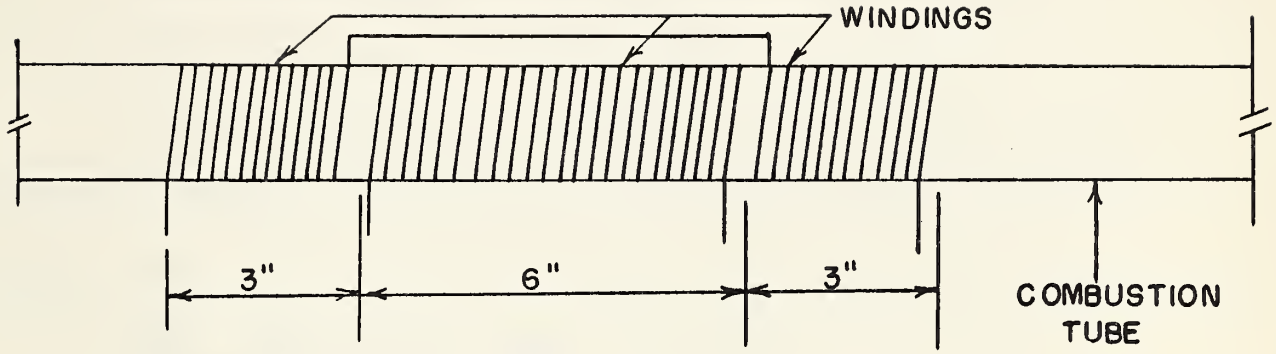

FIGURE 10- FURNACE WINDING ARRANGEMENT

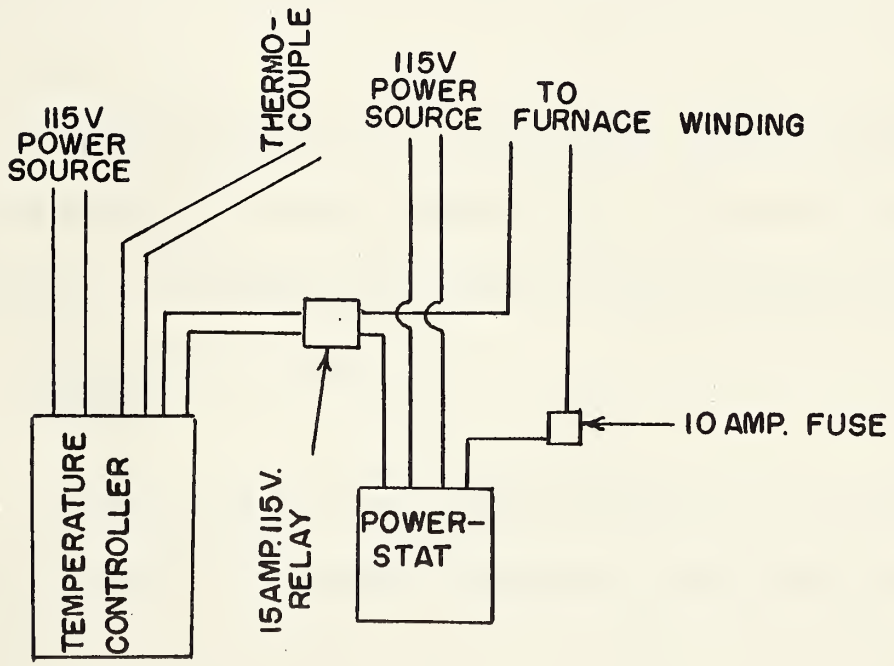

FIGURE 11- WIRING DIAGRAM FOR TEMPERATURE CONTROLLER AND POWERSTAT

APPENDIX III

SO_3 DETERMINATION

The reaction between the SO_2 and the iodine solution is,

$$H_2O + SO_2 + I_2 = 2I^- + SO_3 + 2H^+$$

If 60.0 ml. of SO_2 were collected in 175 ml. of iodine solution at 21°C and 700 mm. of Hg, then the concentration of SO_2 in the iodine solution was

$$\frac{60}{22400} \times \frac{700}{700} \times \frac{273}{294} \times \frac{1000}{175} = 1.31 \times 10^{-2}$$

The hydrogen ion concentration is twice the sulfur dioxide concentration so the hydrogen ion concentration was 2.62×10^{-2} moles/liter.

If the starting pH was 6.6 and 62.45 ml. of 0.1 N NaOH were used to bring the final solution back to this pH. Then the hydrogen ion concentration of the solution after the experiment has taken place was

$$\frac{62.45 \times 0.1}{237.45} = 2.63 \times 10^{-2}$$

By comparing this figure with hydrogen ion concentration due to the SO_2 reaction it is seen that a negligible amount of SO_3 was formed.

APPENDIX IV

CALCULATIONS MADE FROM SO_2 DETERMINATIONS

A sample calculation made from SO_2 determination is as follows:

$$Sb_2S_3 + 9/2O_2 = Sb_2O_3 + 3SO_2$$

Atomic Wt. = 339.7 291.5 192.2

1 mg. y mg. x mg.

$$\frac{1}{339.7} = \frac{x}{192.2}$$

$$x = \frac{192.2}{339.7} = 0.565$$

Therefore 1 mg. of Sb_2S_3 oxidizes producing 0.565 mg. of SO_2. 0.565 mg. of $SO_2 = \frac{565 \times 10^{-6}}{64.1} = 8.83 \times 10^{-6}$ moles of SO_2. At standard temperature and pressure,

$$V = \frac{nRT}{p} = \frac{8.83 \times 10^{-6} \times 82.06 \times 273}{1} = 0.197$$

Therefore 0.565 mg. of SO_2 = 0.197 ml. of SO_2 at standard temperature and pressure. At the experimental conditions, namely, 21°C and 700 mm.Hg (atmospheric pressure at Edmonton)

$$V = \frac{760 \times 0.197 \times 294}{700 \times 273} = 0.230$$

Therefore 0.565 mg. of SO_2 = 0.230 ml. of SO_2 at 21°C and 700 mm. Hg. Thus 1 mg. of Sb_2S_3 oxidizes producing 0.230 ml. of SO_2.

$$\frac{1}{339.7} = \frac{y}{291.5}$$

$$y = \frac{291.5}{339.7} = 0.860$$

Therefore 1 mg. of Sb_2S_3 oxidizes producing 0.860 mg. of Sb_2O_3.

$$Sb_2S_3 + 5O_2 = Sb_2O_4 + 3SO_2$$

339.7 307.5 192.2

1 mg. z mg.

$$\frac{1}{339.7} = \frac{z}{307.5}$$

$$z = \frac{307.5}{339.7} = 0.905$$

Therefore 1 mg. of Sb_2S_3 oxidizes producing 0.905 mg. of Sb_2O_4

$$Sb_2S_3 + 11/2O_2 = Sb_2O_5 + 3SO_2$$

339.7 323.5 192.2

1 mg. w mg.

$$\frac{1}{339.7} = \frac{w}{323.5}$$

$$w = \frac{323.5}{339.7} = 0.953$$

Therefore 1 mg. of Sb_2S_3 oxidizes producing 0.953 mg. of Sb_2O_5.

For the test at 350°C, gas flow of 50 ml./min. and oxygen partial pressure of 35 mm. of Hg, the actual sample weight loss was 19.5 mg. and the volume of SO_2 collected was 22.64 ml.

Weight of Sb_2S_3 oxidized = $\frac{22.64}{0.230}$ = 98.3 mg.

Total possible amount of Sb_2O_3 that could have been formed

= 98.3 x 0.860 = 84.6 mg.

Total possible amount of Sb_2O_4 that could have been formed

= 98.3 x 0.905 = 89.0 mg.

Total possible amount of Sb_2O_5 that could have been formed

= 98.3 x 0.953 = 93.7 mg.

Theoretical sample weight loss if Sb_2O_3 was the only oxide produced and it all remained on the sample was 98.3 - 84.6 = 13.7 mg.

Theoretical sample weight loss if Sb_2O_4 was the only oxide produced and it all remained on the sample was 98.3 - 89.0 = 9.3 mg.

Theoretical sample weight loss if Sb_2O_5 was the only oxide produced and it all remained on the sample was 98.3 - 93.7 = 4.6 mg.

The results of these calculations for all of the experiments run are shown in Table 8.

TABLE 8 - RESULTS OF CALCULATIONS MADE FROM SO_2 DETERMINATIONS

Gas Flow ml/min.	Oxygen Partial Pressure mm. Hg.	Temp. °C	Sample Wt. Loss mg.	Volume of SO_2 ml.	Sb_2S_3 Oxidized mg.	Sb_2O_3 Formed mg.	Sb_2O_4 Formed mg.	Sb_2O_5 Formed mg.	Theoretical Wt. Loss If Sb_2O_3 Formed mg.	Theoretical Wt. Loss If Sb_2O_4 Formed mg.	Theoretical Wt. Loss If Sb_2O_5 Formed mg.
5	175	300	7.8	6.41	27.9	24.0	25.2	26.6	3.9	2.7	1.3
		350	12.2	10.08	43.9	37.8	39.8	41.9	6.1	4.1	2.0
		400	47.5	19.74	85.6	73.6	77.5	81.6	12.0	8.1	4.0
		400	52.2	37.51	163	140	148	155	23	15	8
10	84	300	5.4	5.09	22.2	19.1	20.1	21.2	3.1	2.1	1.0
		350	14.9	10.94	47.4	40.8	42.9	45.2	6.6	4.5	2.2
		400	44.6	35.21	153	132	138	146	21	15	7
		400	53.8	53.00	230	198	208	219	32	22	11
10	105	300	10.2	7.32	31.8	27.4	28.8	30.3	4.4	3.0	1.5
		350	48.9	29.17	127	109	115	121	18	12	6
		400	61.0	45.13	196	169	177	187	27	19	9
		450	122.0	89.01	387	333	350	369	54	37	18
		450	80.4	75.38	327	281	296	312	46	31	15
10	147	300	2.1	1.16	50.2	43.2	45.5	47.9	7.0	4.7	2.3
		350	4.3	28.72	125	108	113	119	17	12	6
		400	43.7	28.88	126	108	114	120	18	12	6
		450	104.5	81.02	352	302	318	336	50	34	16
		450	157.8	125.01	544	468	492	518	7.6	52	26
		560	70.7	20.43	88.7	76.3	80.3	84.6	12.4	8.4	4.1
		600	60.5	39.40	171	147	155	163	24	16	8
		650	514.7	197.39	856	736	775	813	120	81	43
		700	567.5	282.59	1226	1055	1110	1170	171	116	56
		750	526.5	359.99	1565	1345	1415	1490	220	150	75
10	175	300	14.1	9.82	42.7	36.7	38.6	40.7	6.0	4.1	2.0
		350	41.7	54.22	236	203	214	225	33	22	11
		400	40.2	32.52	141	121	128	134	20	13	7
		450	168.7	132.28	573	493	519	546	80	54	27
		450	90.5	101.57	441	379	399	420	62	42	21

TABLE 8 (CONT'D) RESULTS OF CALCULATIONS MADE FROM SO_2 DETERMINATIONS

Gas Flow ml/min.	Oxygen Partial Pressure mm. Hg.	Temp. °C	Sample Wt. Loss mg.	Volume Of SO_2 ml.	Sb_2S_3 Oxidized mg.	Sb_2O_3 Formed mg.	Sb_2O_4 Formed mg.	Sb_2O_5 Formed mg.	Theoretical Wt. Loss If Sb_2O_3 Formed mg.	Theoretical Wt. Loss If Sb_2O_4 Formed mg.	Theoretical Wt. Loss If Sb_2O_5 Formed mg.
10	210	300	6.0	7.17	31.2	25.8	28.2	29.8	5.4	3.0	1.4
		350	32.5	42.12	183	157	166	174	24	17	9
		350	55.3	64.82	282	242	255	269	40	27	13
10	245	300	7.0	10.51	45.7	39.3	41.4	43.6	6.4	4.3	2.1
		350	24.5	37.98	165	142	149	157	23	16	8
		400	61.7	49.77	217	187	196	207	30	21	10
		400	77.3	74.31	324	278	293	309	46	31	15
25	147	300	5.6	5.98	25.9	22.2	23.4	24.7	3.7	2.5	1.2
		350	13.2	17.00	73.9	63.5	66.9	70.5	10.4	7.0	3.4
		400	47.7	51.24	223	192	202	213	31	21	10
		400	59.6	64.38	280	241	254	267	39	26	13
50	35	300	3.2	3.39	23.4	20.1	21.2	22.3	3.3	2.2	1.1
		350	20.8	24.35	106	91.1	96.0	101	14.9	10.0	5
		350	19.5	22.64	98.3	84.6	89.0	93.7	13.7	9.3	4.6
		700	510.1	73.58	320	275	290	305	45	30	15
50	147	300	7.8	11.73	51.0	43.9	46.2	48.7	7.1	4.8	2.3
		350	43.5	45.43	198	170	179	189	28	19	9
		350	45.3	56.67	247	212	223	236	35	24	11
50	235	300	11.0	15.65	68.1	58.6	61.7	64.9	9.5	6.4	3.2
		350	43.6	64.80	282	242	255	268	40	27	14
18600	0.05	300	10.5	29.51	128	110	116	122	18	12	6
		350	4.5	48.90	212	182	192	202	30	20	10
		400	15.9	49.75	216	186	195	206	30	21	10
		450	20.4	84.79	369	317	334	352	52	35	17
		500	37.2	137.29	597	514	541	569	83	56	28

TABLE 9 - RATE OF SULFUR DIOXIDE PRODUCTION

Gas Flow ml./min.	Partial Pressure Of Oxygen mm. Hg.	Oxygen Concentration moles/liter	Temperature °C	Sample Area $cm.^2$	Volume Of SO_2 ml./hr.	Rate of SO_2 Production $ml./hr.cm.^2$
5	175	95.4	300	3.61	6.41	1.78
			350	3.61	10.08	2.80
			400	3.61	19.74	5.48
			400	6.06	37.51	6.19
10	84	45.8	300	4.52	5.09	1.13
			350	4.52	10.94	2.42
			400	4.52	35.21	7.80
			400	6.33	53.00	8.38
10	105	57.2	300	8.90	7.32	0.82
			350	8.90	29.17	3.28
			400	8.90	45.13	5.07
			450	8.84	89.01	10.0
10	147	80.2	300	5.68	1.16	0.2
			350	5.68	28.72	5.06
			400	5.68	28.88	5.11
			450	6.97	81.02	11.6
			560	1.32	20.43	15.5
			600	1.32	39.40	29.8
			650	1.32	197.39	149.5
			700	1.32	282.59	214
			750	1.32	359.99	273
10	175	95.4	300	8.01	9.82	1.22
			350	8.01	54.22	6.82
			400	7.89	32.52	4.18
			450	7.83	132.28	17.3
			450	4.13	101.57	24.5
10	210	114	300	4.26	7.17	1.68
			350	4.26	42.12	9.93
			350	7.10	64.82	9.13
10	245	134	300	4.90	10.51	2.14
			350	4.90	37.98	7.80
			400	4.13	49.77	12.1
			400	6.45	74.31	11.5
25	147	80.2	300	3.62	5.96	1.65
			350	3.62	17.00	4.73
			400	3.62	51.24	14.4
			400	6.71	64.38	9.60
50	35	191	300	4.77	5.39	1.13
			350	4.77	24.35	2.35
			700	1.32	73.58	55.8
50	147	80.2	300	6.71	11.73	1.75
			350	5.81	45.43	7.82
			350	5.94	56.67	9.54
50	235	134	300	5.40	15.65	2.90
			350	5.40	64.80	12.1
18600	0.05	0.262	300	6.45	29.51	4.57
			350	6.45	48.90	7.63
			400	6.39	49.75	7.79
			450	3.09	84.79	27.5
			500	3.01	137.29	45.6